Supplementary Materials

Cholesterol confers ferroptosis resistance onto myeloid-biased hematopoietic stem cells and prevents irradiation-induced myelosuppression

Liu et al.

Table S1

Antibodies used for flow cytometry (FC)

Antibody	Origin	Catalog number	Assay	Dilution
eFluor 450 Mouse Hematopoietic Lineage Cocktail	eBioscience	Cat# 88-7772-72	FC	1:5
Biotin Mouse Hematopoietic Lineage Cocktail	eBioscience	Cat# 88-7774-75	FC	1:50
FITC Mouse Hematopoietic Lineage Cocktail	eBioscience	Cat# 22-7770-82	FC	1:5
Anti-Mouse Ly-6A/E (Sca-1), PerCP-Cyanine5.5	eBioscience	Cat# 45-5981-82	FC	1:80
Anti-Mouse Ly-6A/E (Sca-1), PE-Cyanine7	eBioscience	Cat# 25-5981-82	FC	1:100
Anti-Mouse CD117 (c-Kit), PE	eBioscience	Cat# 12-1172-83	FC	1:200
Anti-Mouse CD117 (c-Kit), APC-eFluor 780	eBioscience	Cat# 47-1171-82	FC	1:100
Anti-Mouse CD117 (c-Kit), PE-Cyanine7	eBioscience	Cat# 25-1171-82	FC	1:200
Anti-Mouse CD117 (c-Kit), APC	eBioscience	Cat# 17-1171-83	FC	1:100
Anti-Mouse CD34, FITC	eBioscience	Cat# 11-0341-85	FC	1:50
Anti-Mouse CD34, eFluor 660	eBioscience	Cat# 50-0341-82	FC	1:33
Anti-Mouse CD34, BV421	BD Biosciences	Cat# 562608	FC	1:40

Anti-Mouse CD135 (Flk2), BV421	eBioscience	Cat# 12-1351-82	FC	1:40
Anti-Mouse CD135 (Flk2), PE	eBioscience	Cat# 12-1351-82	FC	1:33
Anti-Mouse CD135 (Flk2), APC	eBioscience	Cat# 17-1351-82	FC	1:33
Anti-Mouse CD34, Biotin	eBioscience	Cat# 13-0341-85	FC	1:50
Anti-Mouse CD135, Biotin	eBioscience	Cat# 13-1351-85	FC	1:50
Anti-human/mouse CD45R (B220), APC-eFluor 780	eBioscience	Cat# 47-0452-82	FC	1:160
Anti-mouse CD127, PE	eBioscience	Cat# 12-1271-82	FC	1:80
Anti-mouse CD16/32, PE- Cyanine7	eBioscience	Cat# 25-0161-82	FC	1:80
Anti-Mouse CD45R (B220), APC-eFluor™ 780	eBioscience	Cat# 47-0452-80	FC	1:40
Anti-Mouse CD3e, FITC	eBioscience	Cat# 11-0031-85	FC	1:100
Anti-Mouse Ly-6G (Gr-1), PE	eBioscience	Cat# 12-5931-82	FC	1:667
Anti-Mouse CD11b (Mac-1), APC	eBioscience	Cat# 17-0112-83	FC	1:80
Anti-Mouse CD45, eFluor 450	eBioscience	Cat# 48-0451-82	FC	1:40
Anti-Mouse CD150, PE	Biolegend	Cat# 115904	FC	1:100

Anti-Mouse CD150, PE- Cyanine7	eBioscience	Cat# 25-1502-82	FC	1:40
Anti-Mouse CD150, Super Bright™ 645	eBioscience	Cat# 64-1502-82	FC	1:40
Anti-Mouse CD48, FITC	eBioscience	Cat# 11-0481-85	FC	1:200
Anti-Mouse CD48, APC	eBioscience	Cat# 17-0481-82	FC	1:100
Anti-Mouse CD48, eFluor 450	eBioscience	Cat# 48-0481-82	FC	1:40
Anti-Mouse CD48, Super Bright™ 702	eBioscience	Cat# 67-0481-82	FC	1:100
Anti-Mouse LDLR, FITC	eBioscience	Cat# MA5-40965	FC	1:10
Anti-Mouse LDLR, PerCP	eBioscience	MA5-40964	FC	1:10
LDLR Recombinant Rabbit Monoclonal Antibody	eBioscience	Cat# MA5- 29725	FC	1:100
Anti-Phospho-mTOR (Ser2448) Monoclonal Antibody (MRRBY), eFluor™ 450	eBioscience	Cat#48-9718-42	FC	1:20
Anti-Phospho-mTOR (Ser2448) Monoclonal Antibody (MRRBY), eFluor™ 660	eBioscience	Cat#50-9718-42	FC	1:20
Anti-Human/Mouse phospho-AKT (S473), eFluor 450	eBioscience	Cat# 48-9715-42	FC	1:20
Transferrin Receptor Monoclonal Antibody (R17217.1.4), PE	eBioscience	Cat# MA5-17924	FC	1:10

Anti-Glutathione Peroxidase 4 antibody	Abcam	Cat# ab125066	FC	1:100
Anti-4 Hydroxynonenal antibody	Abcam	Cat# ab46545	FC	1:150
Anti-Malondialdehyde antibody	Abcam	Cat# ab27642	FC	1:100
Anti-LPCAT3 antibody	Abcam	Cat# ab232958	FC	1:40
Anti-Ferritin antibody [EPR3004Y]	Abcam	Cat# ab75973	FC	1:50
Anti-SCD1 antibody [EPR21963]	Abcam	Cat# ab236868	FC	1:500
Goat anti- Rabbit IgG(H+L) Cross-Adsorbed Secondary Antibody, Alexa Fluor 488	Thermo Fisher Scientific	Cat# A-11008	FC	1:2000
Goat anti-Rabbit IgG (H+L) Highly Cross-Adsorbed Secondary Antibody, Alexa Fluor 594	Thermo Fisher Scientific	Cat# A-11037	FC	1:2000
ATF4 Recombinant Rabbit Monoclonal Antibody (SD20-92)	Thermo Fisher Scientific	Cat# MA5-32364	FC	1:50
SLC7A11 Polyclonal Antibody	Thermo Fisher Scientific	Cat# PA1-16893	FC	1:50
SREBP1 Polyclonal antibody	Thermo Fisher Scientific	Cat# PA5-120378	FC	1:100
ACSL4 Recombinant Rabbit Monoclonal Antibody (JE56-33)	Thermo Fisher Scientific	Cat# MA5-42523	FC	1:50

ALOX15 Monoclonal Antibody (OTI7H6)	Thermo Fisher Scientific	Cat# MA5-25891	FC	1:100

Table S2

Primers for mRNA expression analysis

Gene	Forward primer (5'-3')	Reverse primer (5'-3')
Ldlr	AGCAGGAGGGAGTCGAGAC	GTTCCTAGCCGGAGATCGC
Srebf2	GCAGCAACGGGACCATTCT	CCCCATGACTAAGTCCTTCAACT
Hmgcr	TCTGTTGTGAACCATGTGACTTC	AGCTTGCCCGAATTGTATGTG
Hprt	TCAGTCAACGGGGGACATAAA	GGGGCTGTACTGCTTAACCAG

Table S3

Gene id						
Abca1	Apon	Cyp11b2	Fgf1	Lcat	Npc2	Soat2
Abca2	App	Cyp27a1	Fgl1	Ldlr	Nsdhl	Sod1
Abca5	Arv1	Cyp39a1	Fmo5	Ldlrap1	Pcsk9	Sqle
Abcg1	Cat	Cyp46a1	G6pd2	Lepr	Pctp	Srebf1
Abcg4	Cebpa	Cyp51	G6pdx	Lima1	Pex2	Srebf2
Acadl	Cel	Cyp7a1	Gba	Lipc	Pmp22	Sult2b1
Acadvl	Ces1b	Cyp7b1	Gba2	Lipe	Pmvk	Thrb
Akr1d1	Ces1c	Dgat2	Gnb3	Lmf1	Pon1	Tm7sf2
Angptl3	Ces1d	Dgkq	Hdlbp	Lpcat3	Por	Tnfsf4
Aplp2	Ces1e	Dhcr24	Hmgcr	Lrp1	Prkaa1	Tsku
Apoa1	Ces1f	Dhcr7	Hmgcs1	Lrp5	Prkaa2	Ttc39b
Apoa2	Ces1g	Ebp	Hmgcs2	Lss	Saa1	Ttc39d
Apoa4	Cftr	Ephx2	Hnf1a	Mbtps1	Sc5d	Vldlr
Apoa5	Ch25h	Erlin1	Hsd17b7	Mt3	Scap	
Apob	Cln6	Erlin2	Hsd3b7	Mttp	Scarb1	
Apobr	Cln8	Fdft1	Idi2	Mvd	Scp2	
Apoc1	Cubn	Fdps	Il4	Mvk	Sec14l2	
Apoc3	Cyb5r3	Fdx1	Insig1	Nfe2l1	Serpina12	
Apoe	Cyp11a1	Fdxr	Insig2	Npc1	Smpd1	
Apof	Cyp11b1	Fech	Lbr	Npc1l1	Soat1	

Figure S1

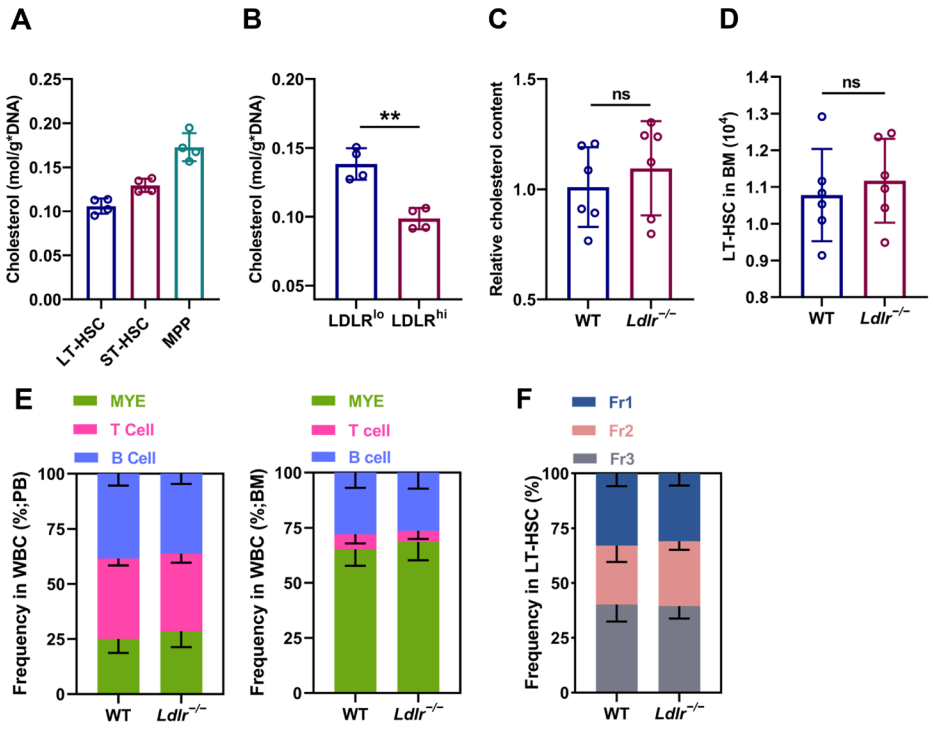

Fig. S1. High levels of cholesterol favor maintenance and myeloid bias of HSCs. (A) Intracellular cholesterol contents in LT-HSCs, ST-HSCs and MPPs as detected by an Amplex™ Red Cholesterol Assay Kit (n = 4). (B) Intracellular cholesterol contents in LDLR^{lo} and LDLR^{hi} LT-HSCs as detected by an Amplex™ Red Cholesterol Assay Kit (n = 4). (C) Flow cytometric analysis of intracellular cholesterol contents in BM LT-HSCs of WT and *Ldlr*$^{-/-}$ mice (n = 6). (D) Flow cytometric analysis of LT-HSC pool size in WT and *Ldlr*$^{-/-}$ mice (n = 6). (E) Frequencies of T cells, B cells and myeloid cells in PB and BM of WT and *Ldlr*$^{-/-}$ mice (n = 6). (F) Flow cytometric analysis of frequency of LT-HSC subpopulations in WT and *Ldlr*$^{-/-}$ mice (n = 6). Data are mean ± SD. n.s., *p < 0.05, **p < 0.01. not significant. two-tailed unpaired Student's t-test.

Figure S2

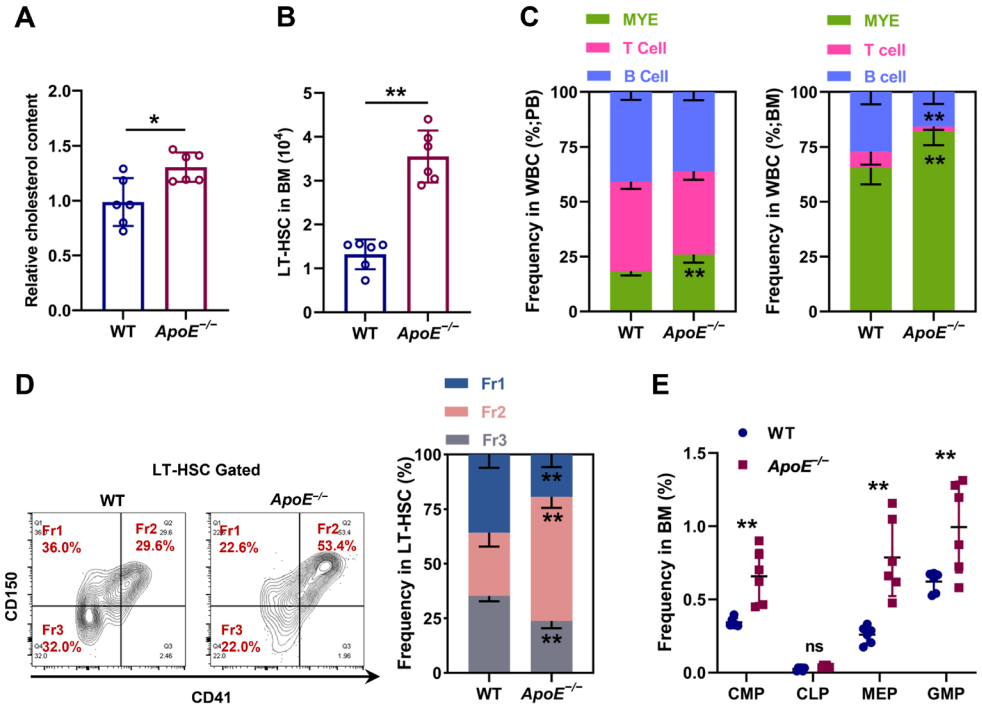

Fig. S2. Hematopoietic phenotype of *ApoE*$^{-/-}$ mice. (A) Flow cytometric analysis of intracellular cholesterol contents in BM LT-HSCs of WT and *ApoE*$^{-/-}$ mice ($n = 6$). (B) Flow cytometric analysis of LT-HSC pool size in WT and *ApoE*$^{-/-}$ mice ($n = 6$). (C) Frequencies of T cells, B cells and myeloid cells in PB and BM of WT and *ApoE*$^{-/-}$ mice ($n = 6$). (D) Flow cytometric analysis of frequency of LT-HSC subpopulations in WT and *ApoE*$^{-/-}$ mice ($n = 6$). (E) Flow cytometric analysis of frequencies of BM CMPs, CLPs, GMPs and MEPs in WT and *ApoE*$^{-/-}$ mice ($n = 6$). Data are mean ± SD. n.s., not significant. *$p < 0.05$, **$p < 0.01$. Two-tailed unpaired Student's *t*-test.

Figure S3

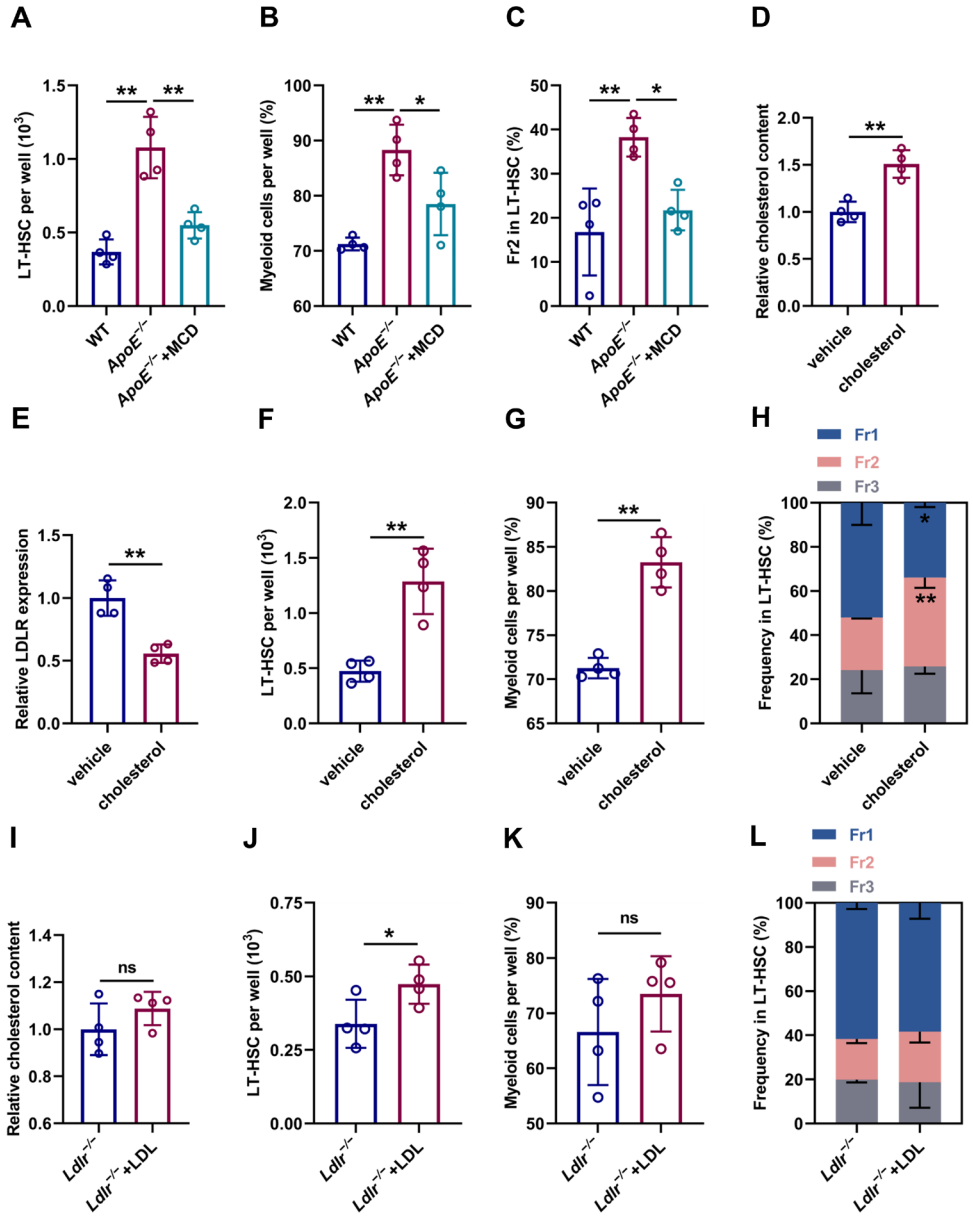

Fig. S3. Cholesterol directly regulates maintenance and lineage differentiation of HSCs. (A) LT-HSC numbers per well in LT-HSC cultures from WT and *ApoE*$^{-/-}$ mice with or without MCD treatment (n = 4). (B) Frequencies of myeloid cell output in LT-HSC cultures from WT and *ApoE*$^{-/-}$ mice with or without MCD treatment (n = 4). (C) Frequency of Fr2 LT-HSCs in LT-HSC cultures from WT and *ApoE*$^{-/-}$ mice with or without MCD treatment (n = 4). (D and E) Flow cytometric analysis of intracellular cholesterol contents (D) and surface expression of LDLR (E) in LT-HSCs with or without

cholesterol treatment ($n = 4$). (F) LT-HSC numbers per well in LT-HSC cultures with or without cholesterol treatment ($n = 4$). (G) Frequencies of myeloid cell output in LT-HSC cultures with or without cholesterol treatment ($n = 4$). (H) Frequency of LT-HSC subpopulations in LT-HSC cultures with or without cholesterol treatment ($n = 4$). (I) Flow cytometric analysis of intracellular cholesterol contents in LT-HSCs from *Ldlr*$^{-/-}$ mice with or without LDL treatment ($n = 4$). (J) LT-HSC numbers per well in LT-HSC cultures from *Ldlr*$^{-/-}$ mice with or without LDL treatment ($n = 4$). (K) Frequencies myeloid cell output in LT-HSC cultures from *Ldlr*$^{-/-}$ mice with or without LDL treatment ($n = 4$). (L) Frequency of LT-HSC subpopulations in LT-HSC cultures from *Ldlr*$^{-/-}$ mice with or without LDL treatment ($n = 4$). Data are mean ± SD. *$p < 0.05$, **$p < 0.01$. Two-tailed unpaired Student's *t*-test unless stated otherwise. One-way ANOVA (A–C).

Figure S4

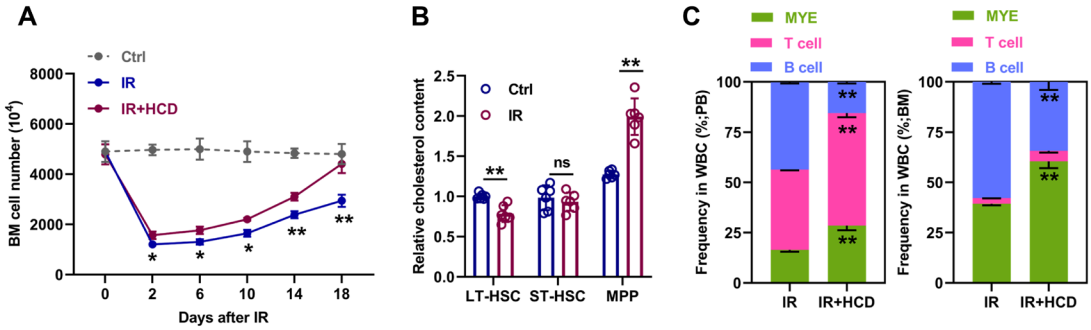

Fig. S4. Cholesterol safeguards HSC maintenance and myeloid regeneration during irradiation-induced myelosuppression. (A) BM cell numbers in CD and HCD mice post IR (n = 4). (B) Flow cytometric analysis of intracellular cholesterol contents in BM HSPCs 24 h post IR (n = 6). (C) Frequencies of T cells, B cells and myeloid cells in PB and BM of CD and HCD mice post IR (n = 6). Data are mean ± SD. n.s., not significant. *p < 0.05, **p < 0.01. Two-tailed unpaired Student's t-test.

Figure S5

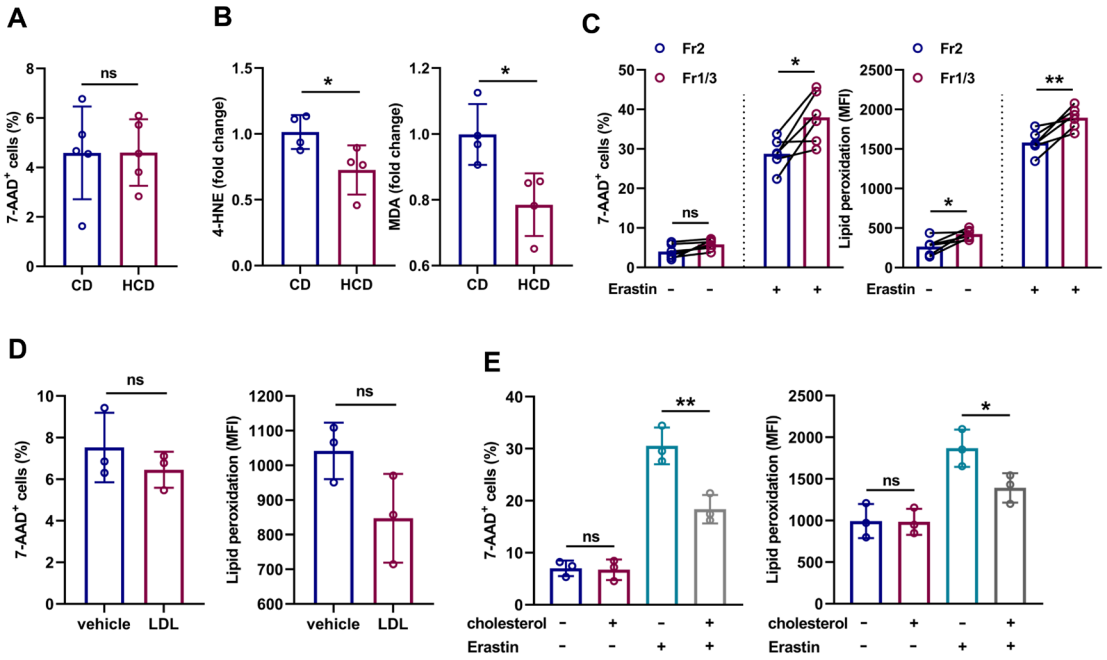

Fig. S5. Cholesterol directly enhances ferroptosis resistance of HSCs. (A) Flow cytometric analysis of cell death in BM LT-HSCs of CD and HCD mice (n = 5). (B) ELISA analysis of 4-HNE and MDA contents in BM LT-HSCs of CD and HCD mice (n = 4). (C) Ferroptosis resistance analysis of Fr2 and Fr1/3 LT-HSCs (n = 6). (D) Cell death and membrane lipid peroxidation in LT-HSCs with or without LDL treatment (n = 3). (E) Ferroptosis resistance analysis of LT-HSCs with indicated treatment (n = 3). Data are mean ± SD. n.s., not significant. *p < 0.05, **p < 0.01, Two-tailed unpaired Student's t-test unless stated otherwise. Two-tailed paired Student's t-test (C). One-way ANOVA (E).

Figure S6

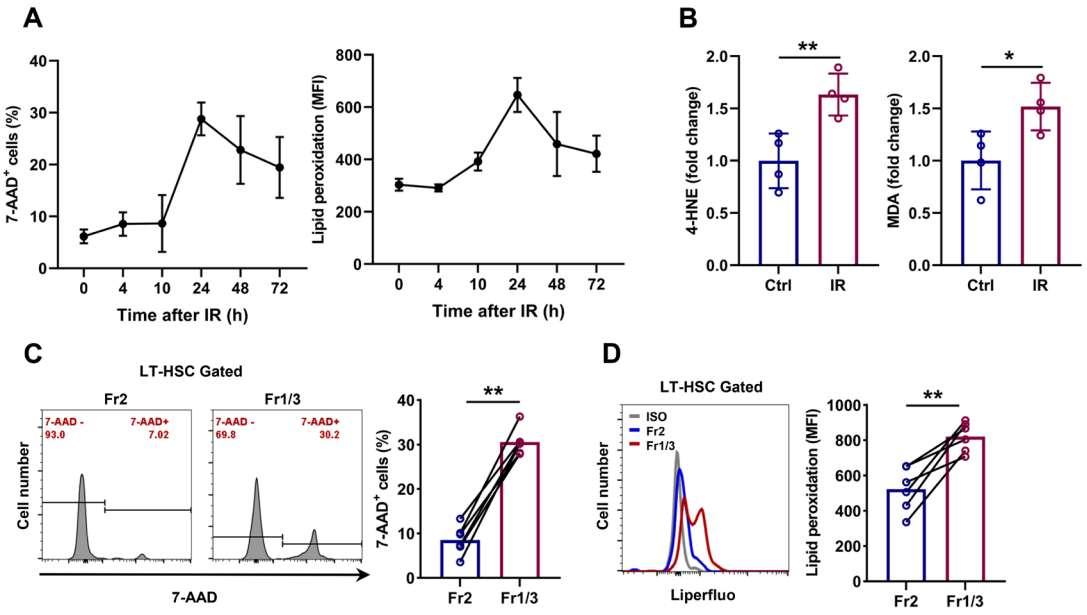

Fig. S6. Cholesterol enhances ferroptosis resistance of HSCs during irradiation-induced myelosuppression. (A) Flow cytometric analysis of cell death and membrane lipid peroxidation in BM LT-HSCs at 24 h post IR (n = 4). (B) ELISA analysis of 4-HNE and MDA contents in BM LT-HSCs at 24 h post IR (n = 4). (C and D) Flow cytometric analysis of cell death (C) and membrane lipid peroxidation (D) in Fr2 and Fr1/3 LT-HSCs 24 h post IR (n = 6). Data are mean ± SD. $^{**}p < 0.01$. Two-tailed unpaired Student's t-test (B). Two-tailed paired Student's t-test (C and D).

Figure S7

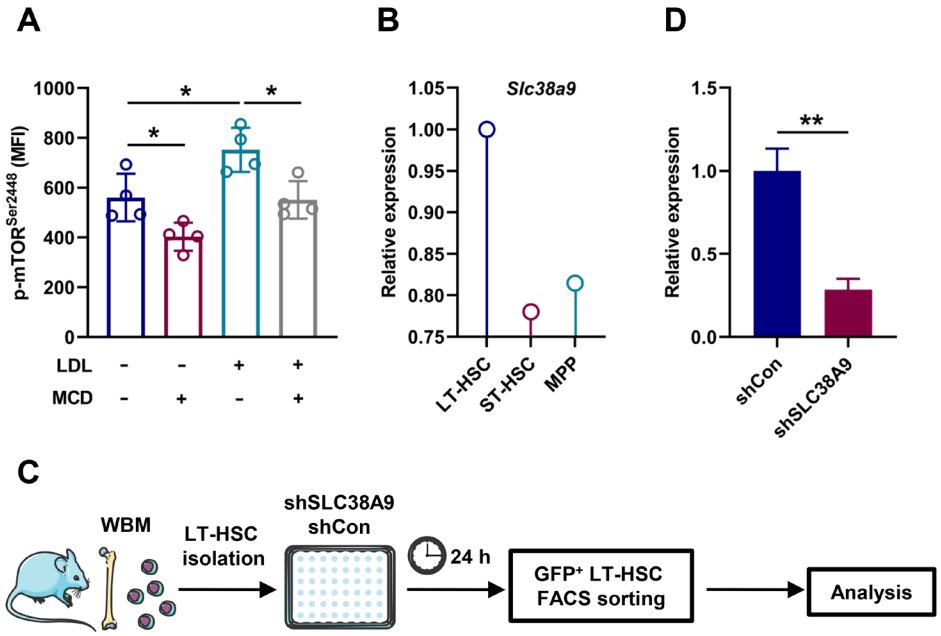

Fig. S7. SLC38A9–mTOR axis mediates cholesterol sensing and signal transduction in HSCs. (A) Flow cytometric analysis of p-mTOR^{Ser2448} protein levels in LT-HSCs with indicated treatment *(n* = 4). (B) Relative mRNA expression of *Slc38a9* based on a published transcriptome database of HSPCs (ArrayExpress: E-MTAB-3079). (C) The protocol for lentiviral transduction and following treatment. (D) Relative *Slc38a9* mRNA expression of *Slc38a9* in LT-HSCs after lentiviral transduction. Data are mean ± SD. *$p < 0.05$, **$p < 0.01$. One-way ANOVA (A), two-tailed unpaired Student's *t*-test (D).

Figure S8

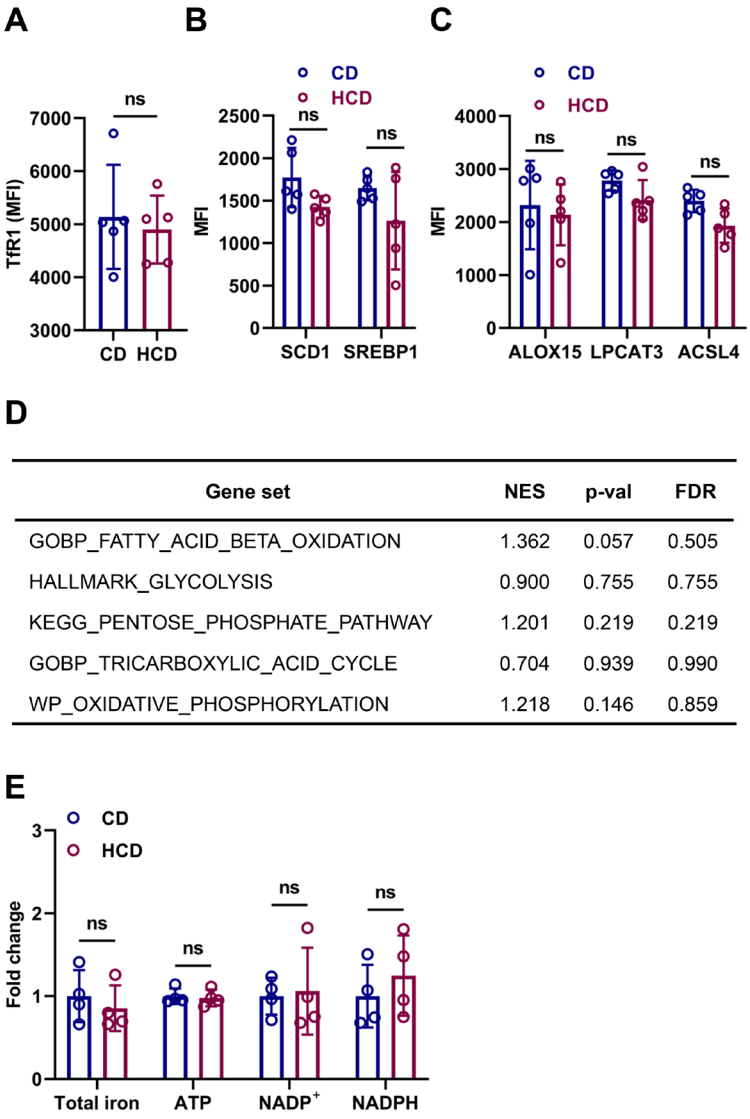

Gene set	NES	p-val	FDR
GOBP_FATTY_ACID_BETA_OXIDATION	1.362	0.057	0.505
HALLMARK_GLYCOLYSIS	0.900	0.755	0.755
KEGG_PENTOSE_PHOSPHATE_PATHWAY	1.201	0.219	0.219
GOBP_TRICARBOXYLIC_ACID_CYCLE	0.704	0.939	0.990
WP_OXIDATIVE_PHOSPHORYLATION	1.218	0.146	0.859

Fig. S8. mTOR has no impact on iron import, MUFA generation, lipid peroxide generation and energy metabolism in LT-HSCs of HCD mice. (A–C) Flow cytometric analysis of TfR1, SREBP1/SCD1 and ACSL4/LPCAT3/ALOX15 protein levels in BM LT-HSCs of CD and HCD mice *(n* = 5). (D) GSEA of indicated gene sets in BM LT-HSCs of HCD mice. (E) Intracellular total iron, ATP, $NADP^+$ and NADPH levels in BM LT-HSCs of CD and HCD mice (*n* = 4). Data are mean ± SD. **p* < 0.05, ***p* < 0.01, Two-tailed unpaired Student's *t*-test.

Figure S9

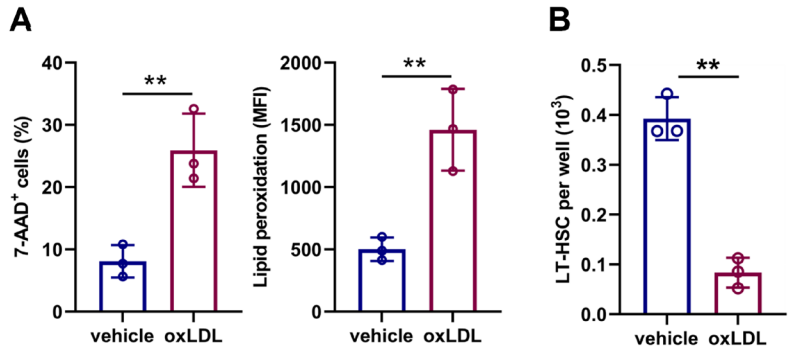

Fig. S9. oxLDL enhances ferroptosis sensitivity and impaires maintenance of LT-HSCs *in vitro*. (A) Cell death and membrane lipid peroxidation of LT-HSCs with or without oxLDL treatment ($n = 3$). (B) LT-HSC numbers per well in LT-HSC cultures with or without oxLDL treatment ($n = 3$). Data are mean ± SD. *$p < 0.05$, **$p < 0.01$, two-tailed unpaired Student's *t*-test.